Raft Polymerization of *N*,*N*-Dimethylacrylamide Utilizing Novel Chain Transfer Agents Tailored for High Reinitiation Efficiency and Structural Control†

Michael S. Donovan, Andrew B. Lowe, Brent S. Sumerlin, and Charles L. McCormick*

Department of Polymer Science, The University of Southern Mississippi, Box 10076, Hattiesburg, Mississippi 39406-0076

Received November 28, 2001; Revised Manuscript Received February 28, 2002

ABSTRACT: The syntheses of the novel acrylamido-based RAFT chain transfer agents (CTAs) *N*,*N*-dimethyl-*s*-thiobenzoylthiopropionamide (TBP, **1c**) and *N*,*N*-dimethyl-*s*-thiobenzoylthioacetamide (TBA, **1d**) for the controlled polymerization of *N*,*N*-dimethylacrylamide (DMA) are described. The results from a comparative study of **1c** and **1d** with two CTAs previously reported for the RAFT polymerization of DMA (benzyl dithiobenzoate (BDB, **1a**) and cumyl dithiobenzoate (CDB, **1b**)) are disclosed and demonstrate the effectiveness of the newly reported CTAs. Polymerizations at CTA/I ratios of 5/1 yield poly(*N*,*N*-dimethylacrylamide) (PDMA) homopolymers with high molecular weight impurity (**1b**−**1d**) or bimodal molecular weight distributions (**1a**). The high molecular weight impurity observed in polymerizations mediated by **1b**−**1d** has been attributed to species arising from bimolecular termination reactions, as determined by multiple detector size exclusion chromatography (SEC). The bimodality observed for **1a**-mediated polymerizations is due to the presence of two distinct "active" species, as determined by end group analysis using SEC. We show that it is possible to reduce/eliminate the high molecular weight impurity for **1b**−**1d**-mediated polymerizations simply by increasing the CTA/I ratio to 80/1. Under these conditions, **1a**-mediated polymerization still yields a bimodal molecular weight distribution. The differences in the efficiency of the CTAs **1a**−**1d** are rationalized in terms of their structural and electronic characteristics and their relative fragmentation/reinitiation efficiencies.

Introduction

Recent advances in controlled free radical polymerization have allowed the tailoring of macromolecules with complex architectures including block, graft, comb, and star structures with predetermined molecular weight and narrow molecular weight distributions. One of the most versatile methodologies that permits the selection of a wide range of monomer types and convenient synthetic procedures is reversible addition−fragmentation chain transfer (RAFT) polymerization.[1] The process, illustrated in Scheme 1, involves conventional free radical polymerization in the presence of a chain transfer agent (CTA) such as a dithioester. The degenerative transfer between the growing radicals and the thiocarbonylthio group provides "living" or controlled chain growth. A wide range of structurally diverse CTAs has been reported including dithioesters,[2] trithiocarbonates,[3] dithiocarbamates,[4] xanthates,[5] and phosphoryl-/(thiophosphoryl)dithioformates.[6] Key to structural control in the RAFT process is careful selection of appropriate monomers, initiators, and CTAs.

As part of our continuing research on water-soluble (co)polymers with such applications as pharmaceuticals, cosmetics, and responsive rheology modifiers, we have been especially interested in the synthesis of macro-CTAs and block copolymers from neutral hydrophilic or ionic monomers. For example, we recently reported the controlled synthesis of pH-responsive amphiphillic block copolymers via aqueous RAFT utilizing styrenic and acrylamido-based monomers.[7] However, to date, there are no prior reports regarding the influence of CTA architecture on the polydispersity and molecular weight control of acrylamido-based monomers.

The synthesis of poly(*N*,*N*-dimethylacrylamide) (PDMA) in a controlled fashion, i.e., with predetermined molecular weights and narrow molecular weight distributions, is necessary for the preparation of materials (homopolymers, block copolymers, etc.) for model studies and elucidation of structure−property relationships. This is particularly important given the commercial importance of *N*,*N*-dimethylacrylamide (DMA) for pharmaceutical/personal care-type applications.

To date, the controlled polymerization of DMA has proven challenging using techniques such as atom transfer radical polymerization or stable free radical polymerization. Herein we disclose the successful controlled RAFT polymerization of DMA utilizing two novel CTAs *N*,*N*-dimethyl-*s*-thiobenzoylthiopropionamide and *N*,*N*-dimethyl-*s*-thiobenzoylthioacetamide (**1c** and **1d**, Scheme 1) in which R has been designed to reflect the electronic and structural characteristics of the propagating chain. It will be demonstrated that **1c** allows for excellent control of molecular weight and molecular weight distribution presumably by the rapid establishment of chain equilibration in the RAFT process (step IV, Scheme 1). This is achieved through the efficient reinitiation of the polymerization by the leaving group upon fragmentation, as illustrated in steps II and III. By comparative polymerizations using previously reported CTAs **1a** and **1b** and the novel CTAs **1c** and **1d**, it will be shown that the structural characteristics of the CTA are critical for achieving narrow unimodal molecular weight distributions as well as molecular weight control in the polymerization of DMA. The previously reported CTAs show less than ideal behavior

† Paper No. 85 in a series entitled "Water-Soluble Polymers".

* To whom correspondence should be addressed.

10.1021/ma0120714 CCC: $22.00
Published on Web 04/16/2002

Scheme 1. Pathway for Reversible Addition−Fragmentation Chain Transfer Polymerization

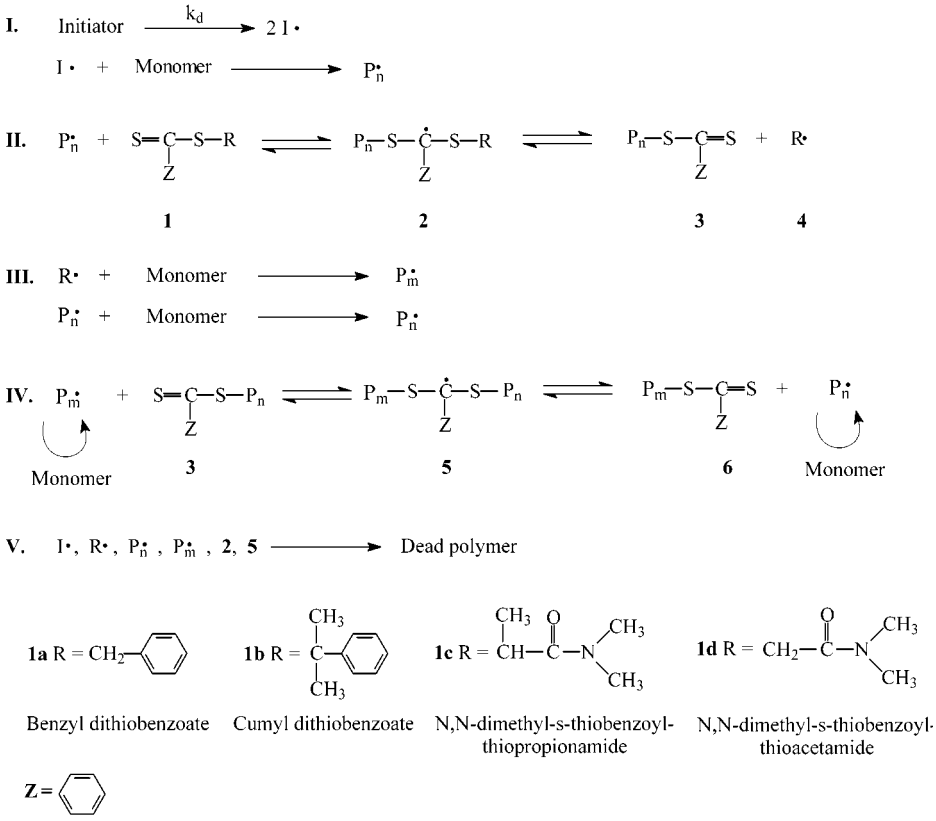

including extended preequilibrium periods (**1a**, **1b**) and bimodal molecular weight distributions compared to CTAs **1c** and **1d**.

Experimental Section

Materials. All chemicals were purchased from Fischer, Acros, or Aldrich Chemical Companies at the highest purity available and used as received unless stated otherwise. 2,2′-Azobis(isobutyronitrile) (AIBN) was recrystallized from ethanol, and carboxymethyl dithiobenzoate was recrystallized from benzene. Benzene and *N*,*N*-dimethylacrylamide were dried over calcium hydride, vacuum-distilled, and purged with nitrogen prior to use.

Synthesis of *N*,*N*-Dimethyl-2-mercaptopropionamide. The title compound was synthesized in a manner similar to that reported by Bhandari et al.[8] To a 100 mL round-bottomed flask was added 2-mercaptopropionic acid (50.0 mL, 0.56 mol). Dimethylamine (23.9 g, 0.53 mol) was added to the solution while keeping the reaction flask in a water bath. Excess dimethylamine was removed using a water aspirator. The reaction was heated at 110 °C for an extended period, during which time the reaction took on a light yellow color. The product was fractionally distilled under reduced pressure. The major crude fraction, which was collected at approximately 80 °C (0.02 mmHg), was determined to contain 57% of the target compound and 43% acid precursor. The acid impurity was removed by washing with dilute NaOH/CH_2Cl_2. The CH_2Cl_2 was removed using a rotary evaporator and the target compound purified by vacuum distillation (bp 80 °C at 0.02 mmHg). Yield = 45%. ^{1}H NMR ($CDCl_3$) δ (ppm): 1.53 (d, $-CH_3$), 2.11 (s, −SH), 2.99 (s $-CONCH_3$), 3.16 (s, $-CONCH_3$), 3.67 (m, −CH).

Synthesis of *N*,*N*-Dimethyl-2-mercaptoacetamide. *N*,*N*-Dimethyl-2-mercaptoacetamide was synthesized in a fashion similar to *N*,*N*-dimethyl-2-mercaptopropionamide. 2-Thioglycolic acid (50.0 mL, 0.563 mol) was reacted with dimethylamine (23.9 g, 0.53 mol) in the manner reported above. The reaction was allowed to proceed at 110 °C for 5 days. The product was then distilled and purified. The product was purified via vacuum distillation (bp 112 °C at 1.0 mmHg). Yield = 68%. ^{1}H NMR ($CDCl_3$) δ (ppm): 2.41 (s, −SH), 2.99 (s, $-CONCH_3$), 3.08 (s, $-CONCH_3$), 3.36 (m, $-CH_2$).

Synthesis of *N*,*N*-Dimethyl-*s*-thiobenzoylthiopropionamide (TBP, 1c). The title compound was synthesized in a manner similar to *N*,*N*-dimethyl-*s*-thiobenzoylthioacetamide. Carboxymethyl dithiobenzoate (5.00 g, 23.60 mmol) was mixed with deionized water (20 mL) and neutralized with a dilute solution of sodium carbonate to a final volume of 130 mL. Subsequently, *N*,*N*-dimethyl-2-mercaptopropionamide (3.13 g, 15.0 mmol) was added to the sodium carboxymethyl dithiobenzoate solution. After 24 h the contents of the flask were poured into a separatory funnel, and a dark red oil was isolated. The aqueous phase was washed with diethyl ether (30.0 mL) to extract the remaining product. Subsequently, the products were dissolved in diethyl ether (50.0 mL) and washed with deionized H_2O (25.0 mL). The diethyl ether phase was separated and dried over anhydrous sodium sulfate. The solution was filtered and the solvent removed via a rotary evaporator. The product was isolated as deep orange plates by recrystallization from a mixture of methanol/water (3:2 v/v). Yield = 52%; melting point 61−62 °C. ^{1}H NMR (d_6-DMSO) δ (ppm): 1.52 (d, $-CH_3$) 2.88 (s, $-N-CH_3$), 3.08 (s, $-N-CH_3$), 5.04 (m, −CH), 7.50, 7.66, 7.96 (m, −CH). ^{13}C NMR (d_6-DMSO) δ (ppm): 16.54 (CH_3), 35.46 ($N-CH_3$), 36.86 ($N-CH_3$), 47.15 (CH), 126.42, 128.70, 133.04, 143.71 (CH), 169.02 (C=O), 226.46 (CS_2). IR (KBr disk): 1643.1 (C=O); 1039.9 (C=S). CHNS elemental microanalysis for $C_{12}H_{15}NOS_2$: Calculated: C, 56.88%; H, 5.97%; N, 5.53%; S, 25.31%. Found: C, 56.89%; H, 5.74%; N, 5.48%; S, 25.19%.

Synthesis of *N*,*N*-Dimethyl-*s*-thiobenzoylthioacetamide (TBA, 1d). Carboxymethyl dithiobenzoate (30.22 g, 142.0 mmol) was neutralized with a dilute aqueous solution of sodium carbonate. *N*,*N*-Dimethyl-2-mercaptoacetamide (16.28 g, 15.0 mmol) was subsequently added to the sodium carboxymethyl dithiobenzoate solution. The reaction was allowed to proceed for 24 h. The product was subsequently extracted with diethyl ether and dried over anhydrous sodium sulfate. The solution was filtered and the solvent removed via a rotary evaporator. The product was isolated as deep orange needles

by recrystallization from a mixture of methanol/water (3:2 v). Yield = 57%; melting point 63−64 °C. ^{1}H NMR (d_6-DMSO) δ (ppm): 2.88 (s, −N−CH_3), 3.12 (s, −N−CH_3), 4.48 (s, −CH_2), 7.50, 7.66, 7.98 (m, −CH). ^{13}C NMR (d_6-DMSO) δ (ppm): 35.29 (N−CH_3), 36.98 (N−CH_3), 41.008 (CH_2), 126.35, 128.66, 132.88, 144.23 (CH), 165.20 (C═O), 227.29 (CS_2). IR (KBr disk): 1654.6 (C═O); 1045.3 (C═S). CHNS elemental microanalysis for $C_{11}H_{13}NOS_2$: Calculated: C, 55.20%; H, 5.47%; N, 5.85%; S, 26.79%. Found: C, 55.11%; H, 5.37%; N, 5.84%; S, 26.86%.

RAFT Polymerizations. Polymerizations of *N*,*N*-dimethylacrylamide (DMA) in benzene were conducted at 60 °C in flame-sealed ampules equipped with magnetic stir bars, whereas polymerizations in d_6-benzene were performed in flame-sealed NMR tubes. All polymerizations were performed at monomer concentrations of ∼1.93 M in benzene, with AIBN as the free radical initiator. Polymerizations at a CTA/I ratio of 5/1, in d_6-benzene, were performed at an initiator concentration of 9.52×10^{-4} mol, for a target molecular weight of 40 000. Similarly, the polymerizations conducted at a CTA/I ratio of 80/1, in benzene, were performed at an initiator concentration of 6.28×10^{-5} mol, for a target molecular weight of 40 000. The ampules were subjected to three freeze−pump−thaw cycles to remove oxygen from the DMA solutions and were subsequently placed in a preheated water bath or inserted into the NMR spectrometer with the temperature maintained at 60 °C. Termination of the polymerizations was achieved by freezing the reactions in a dry ice/acetone bath. The polymers were isolated by precipitation into hexane, filtered, redissolved in THF, and reprecipitated into hexane. Conversions were determined gravimetrically (polymerizations at a CTA/I ratio of 80/1) or by ^{1}H NMR spectroscopy (polymerizations at a CTA/I ratio of 5/1).

Analytical Techniques. *Size Exclusion Chromatography.* The molecular weights of the homopolymers were determined by size exclusion chromatography (SEC) using PLgel 5 μm Mixed D columns. The mobile phase consisted of HPLC grade DMF. The flow rate was maintained at 0.5 mL min^{-1} using an Agilent 1100 series pump. The SEC detectors included a Wyatt Optilab DSP Interferometric refractometer, a Wyatt DAWN EOS multiangle laser light scattering (MALLS) detector, and a Polymer Labs LC1200 UV/vis detector. The molecular weight and polydispersity data were determined using the Wyatt ASTRA SEC/LS software package.

Other Measurements. The refractive index increment (d*n*/d*c*) of poly(*N*,*N*-dimethylacrylamide) (PDMA) in DMF was measured using a Wyatt Optilab DSP Interferometric refractometer fitted with a syringe pump in flow through mode using a range of polymer concentrations operating at 25 °C at a laser wavelength of 690 nm. ^{1}H NMR spectra were recorded in d_6-DMSO, $CDCl_3$, or d_6-benzene with a Bruker AC-300 spectrometer using a 2 s recycle time. UV−vis spectra for the determination of extinction coefficients were obtained using a Varian Cary 500 scan UV−vis−NIR spectrophotometer in DMF. CHNS elemental microanalyses were performed by MWH Laboratories, Phoenix, AZ.

Results and Discussion

Key Steps in RAFT Polymerization. Scheme 1 reflects the major steps in the RAFT process.[9] Classical initiation (I) is followed by a "preequilibrium" step II in which addition to the thioester **1** results in an intermediate radical species **2** which can fragment either to the active chain radical formed in step I or to R$^\bullet$, which subsequently reacts with monomer in reinitiation (step III) to form a new propagating radical $P_m^\bullet$. The main equilibrium between the dormant polymeric RAFT species **3** and **6** and the $P_m^\bullet$ and $P_n^\bullet$ radicals is illustrated in step IV. The efficient transfer of the dithioester between active and dormant chains is necessary to maintain the "living" character of the polymerization. Bimolecular termination events, including coupling and disproportionation (step V), are always operative to some extent but can be largely eliminated by maintaining appropriate conditions.

The key to controlled RAFT polymerizations is the choice of the CTA. The electronic nature of the Z group influences the relative rates of formation and scission of the radical intermediates **2** and **5**. The phenyl Z group was chosen for these studies based on the success of previous authors in the RAFT polymerization of DMA[1] and other acrylamido-based monomers.[7b,10] The R group should be chosen so that fragmentation of intermediate **2** is facile, and the leaving radical R$^\bullet$ has sufficient potential energy to reinitiate polymerization. The relative rates of addition and fragmentation (and intermediate lifetimes of **2** and **5**) for a variety of monomer/CTA combinations are the focus of extensive research and the subject of current debate.[9,11] However, it is has been established that in order to obtain polymers with low polydispersity and predetermined degrees of polymerization, both the addition and fragmentation in steps II and IV must be fast relative to propagation.[1]

Design of CTAs 1c and 1d for Polymerization of *N*,*N*-Dimethylacrylamide (DMA). Our initial attempts at the polymerization of DMA utilizing **1a** and **1b** were unsatisfactory as evidenced by long inhibition periods and bimodal molecular weight distributions (**1a**). On the basis of a study of available literature,[1b,13] we reasoned that these CTA's did not possess the structural characteristics necessary to rapidly establish the main equilibrium (step IV, Scheme 1). Inefficient fragmentation/reinitiation in steps II and III appeared to be the most likely problem. Therefore, we designed, synthesized, and characterized *N*,*N*-dimethyl-*s*-thiobenzoylthiopropionamide (**1c**) and *N*,*N*-dimethyl-*s*-thiobenzoylthioacetamide (**1d**). Both of these CTAs yield acetamido intermediate radicals in the preequilibrium that are structurally and electronically similar to the propagating chain end of the DMA macroradical (Figure 1). It should be noted also that **1c** possesses a methyl group that should enhance the cleavage of the S−C bond. Comparing the behavior of these CTAs with previously reported **1a** and **1b** was expected to provide insight into the necessary structural characteristics for efficient RAFT polymerizations for acrylamido-based monomers.

Synthesis and Structural Characterization of 1c and 1d. CTAs **1c** and **1d** were prepared via a multistep procedure shown in Scheme 2. 2-Thioglycolic acid and 2-mercaptopropionic acid were both reacted with dimethylamine in the first step to yield the respective intermediate amides. The thiols were then reacted with sodium carboxymethyl dithiobenzoate in a thioester interchange reaction to yield the target CTAs in a facile manner. Compounds **1c** and **1d** were isolated as orange crystals with sharp melting points of 63−64 and 61−62 °C, respectively. Structures were confirmed as detailed in the Experimental Section by CHNS elemental microanalysis and infrared and NMR spectroscopies. The ^{1}H and ^{13}C NMR spectra of **1c** and **1d** are shown in Figure 2.

Preliminary RAFT Polymerization of DMA with 1c. In a preliminary experiment **1c** was evaluated as a novel model CTA for the controlled polymerization of DMA. The polymerization was conducted in d_6-benzene at 60 °C, using AIBN as the free radical initiator, at a CTA/I ratio of 5/1 (see Table 1). This experiment was used to determine the kinetics of polymerization at low conversion values. In Figure 3 are shown the SEC chromatograms (RI response) for aliquots of the polym-

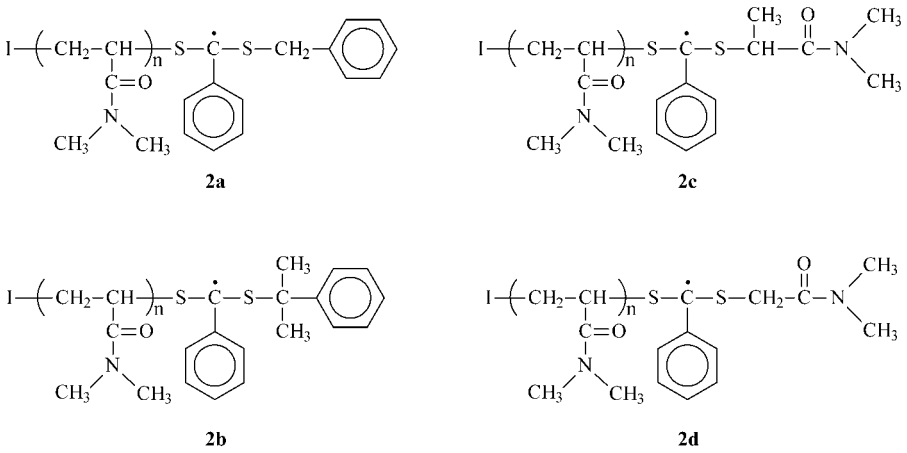

Figure 1. Intermediate radical structures of CTAs **1a**−**1d**.

Scheme 2. Synthetic Route for *N*,*N*-Dimethyl-*s*-thiobenzoylthiopropionamide (1c) and *N*,*N*-Dimethyl-*s*-thiobenzoylthioacetamide (1d)

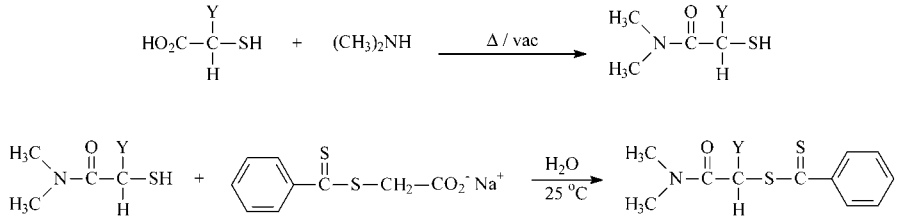

erization at various time intervals (Figure 3a), along with the kinetic plot (Figure 3b) and the molecular weight vs conversion and polydispersity vs conversion plots (Figure 3c).

The SEC chromatograms in Figure 3a clearly show the increase in molecular weight with time. Also noted is the appearance of a higher molecular weight species—evidenced as a shoulder, at extended polymerization time. The kinetic plot in Figure 3b shows first-order behavior, implying a constant number of radicals. The number-average molecular weight increases in a linear fashion with conversion (Figure 3c), at least up to approximately 60%, and is characteristic of a controlled or living process. The polydispersity shows an initial decrease with increasing conversion and then begins to increase slightly. At all times the polydispersity remains low (M_w/M_n < 1.25)—well below the theoretical lowest limit of 1.50 for a conventional free radical polymerization.

A Comparative Study of the RAFT Polymerization of DMA in the Presence of CTAs 1a−1d. RAFT polymerizations of *N*,*N*-dimethylacrylamide (DMA) were conducted in benzene at 60 °C using AIBN as the initiator. Polymerizations were performed in degassed, flame-sealed glass reactors in order to preclude any possible oxidation of the CTAs. Pertinent data including CTA/I ratios, reaction times, conversions, and molecular weights are given in Table 2.

To follow kinetics at short reaction times (and thus evaluate any effects of CTA structure on the preequilibrium in Scheme 1), a series of comparative polymerizations were monitored directly by NMR spectroscopy. CTA/I ratios of 5/1 were utilized with the temperature held constant at 60 °C in d_6-benzene. The spectra were obtained at 15 min intervals for 9 h, with a data acquisition time of 108 s. Conversions at longer time intervals were followed by analyzing aliquots of identical solutions taken from separate flame-sealed ampules heated in a water bath at 60 °C. Polydispersities and absolute molecular weights were determined by size exclusion chromatography in DMF utilizing inline RI, UV, and MALLS detectors. It should be noted that PDMA homopolymers prepared in the absence of CTA (conventional free radical polymerization) typically gelled within 1−2 h and when analyzed by SEC eluted at the void volume of the columns, indicating very high molecular weight, uncontrolled species.

Figure 4 illustrates the respective kinetic plots for the polymerization of DMA with CTAs **1a**−**1d**. The importance of reinitiation following fragmentation in the preequilibrium (step II, Scheme 1) is demonstrated by the notable time intervals required to reach a constant slope in the respective $\ln(M_0/M_t)$ vs time plots. These times are approximately 25 min for the novel CTAs **1c** and **1d** compared to approximately 80 and 100 min for **1a** and **1b**, respectively. This order is in agreement with that expected for reinitiation based on radical reactivity alone. The more stable, bulky cumyl radical from **1b** should add to DMA slower than the primary benzyl radical from **1a** and significantly slower than the acetamido radicals from **1c** and **1d**. This is also consistent with the published reactivity ratios r_1 and r_2 for the styrene/DMA pair[12] of 1.37 and 0.49, respectively.

The lack of conversion early in the polymerization using **1b** has been observed for other monomers. For example, Moad et al.[13] noted the poor initiating ability of the cumyl radical for styrene, which resulted in an induction period of up to 1 h. The kinetic plot with RAFT agent **1a** shows a slightly different trend in which the conversion rate is higher than that of **1b** but is still retarded early in the polymerization, finally reaching a constant value after approximately 80 min. This differ-

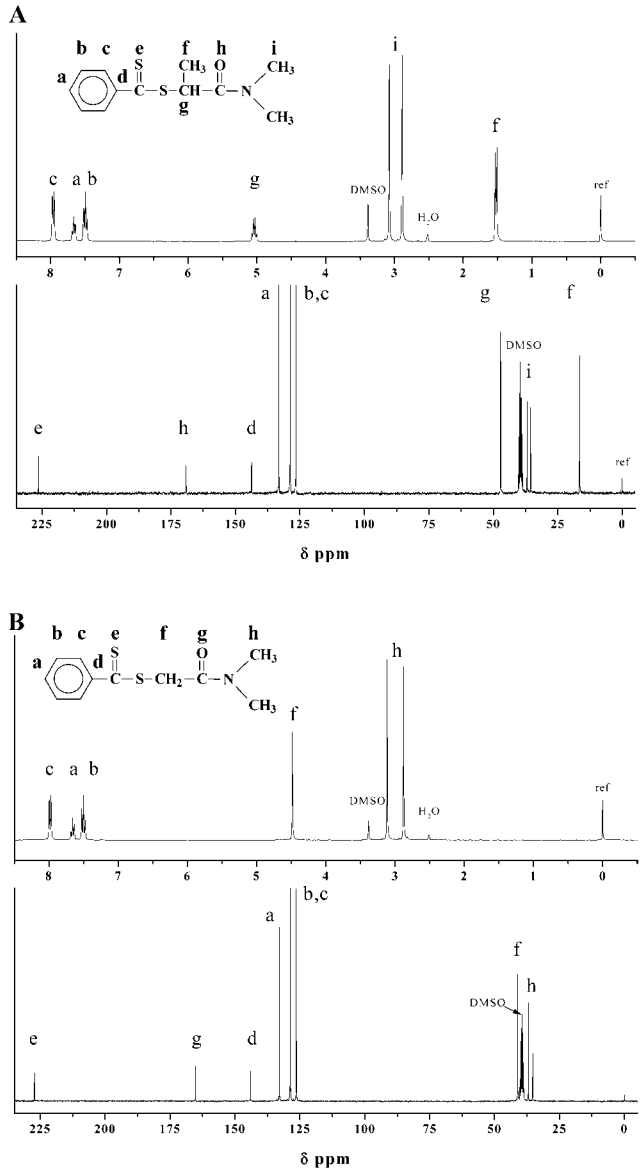

Figure 2. ^{1}H and ^{13}C NMR spectra of (A) CTA **1c** and (B) CTA **1d** in d_6-DMSO.

Table 1. Data from the RAFT Polymerization of DMA with CTA 1c (Target MW = 45 000) in d_6-Benzene at 60 °C Using a CTA/I Ratio of 5/1, [M] = 1.95 M, [CTA] = 4.27 × 10^{-3} M, [I] = 8.46 × 10^{-4} M

CTA	CTA/I	time (min)	% conv	Mn_{Th}	Mn_{SEC}	M_w/M_n
1c	5	100	12	5 400	3 732	1.22
1c	5	296	24	10 800	12 550	1.11
1c	5	550	32	14 400	18 650	1.09
1c	5	1136	53	23 850	31 640	1.11

[a] As determined by ^{1}H NMR spectroscopy, recorded in d_6-benzene. [b] SEC in DMF at room temperature, at a flow rate of 0.5 mL/min, with x2 PL Mixed-D columns, PL UV-1200, Optilab RI, and DAWN EOS detectors.

ence may be attributed to the "hotter" benzyl radical, which is expected to be a better initiating species than the cumyl radical. It is, however, apparent from Figure 1 that both fragmentation and reinitiation should be more balanced with CTAs **1c** and **1d** since the macroradicals from both are nearly identical to the reinitiating fragments ($R^{\bullet}$).

In any event, once the preequilibrium phase of the RAFT process is reached, polymerizations with all four CTAs exhibit a first-order relationship between monomer conversion and polymerization time, at least up to moderately long polymerization times (Figure 4). This first order relationship is maintained in the respective systems up to approximately 55% conversion, after which the rates decrease. The breakdown in "livingness" of these polymerizations, like other controlled free radical processes, is indicative of bimolecular termination events (step V, Scheme 1). These events can be greatly suppressed by increasing the CTA/I ratio as will be discussed later.

Molecular Weight Dependence on CTA Architecture. The theoretical molecular weights (Mn_{Th}) for the polymerizations at CTA/I ratios of 5/1 ranging from 14 to 186 h are listed in Table 2. The Mn_{Th} values, which were determined using eq 1, are shown along with the experimentally determined molecular weights (Mn_{SEC}).

$$MW_{Th} = \frac{[M] \times MW_{mon}}{[CTA]} \times \% \text{ conversion} + MW_{CTA} \quad (1)$$

It can be clearly seen that the latter diverges dramatically from the former with conversion. When comparing the four CTAs at specific reaction times, the best correlation between the Mn_{SEC} and the Mn_{Th} is observed with **1c**. This result is indicative of the importance of the events that take place early in the RAFT mechanism. The similarity between **1c** and $P_n^{\bullet}$ allows all chains to be started early in the RAFT polymerization. For CTAs **1a** and **1b**, the differences between Mn_{Th} and Mn_{SEC} are slightly higher. This result is again consistent with those reported by Moad et al.[13] for the polymerization of styrene with **1b**. The authors noted the poor initiating ability of the cumyl radical for styrene, leading to higher than predicted molecular weights. For **1d**, the molecular weights are also higher than predicted which may be attributed to the low steric strain and relative instability of the leaving group, compared to that of the propagating chain. Upon fragmentation, the primary radical should be an efficient initiator; however, the low steric strain of the R group may result in the preferential expulsion of the propagating polymer ($P_n^{\bullet}$) instead of the $R^{\bullet}$, thereby extending the preequilibrium.

Table 2 indicates that the conversion rates at extended times decrease dramatically due to a reduction in the number of active chains and the low concentration of monomer. Chromatograms (see Figure 5) from the DMA polymerizations using CTAs **1b**−**1d** show evidence of bimolecular radical coupling as determined by the presence of high molecular weight shoulders. Using the MALLS detector, it was determined that these shoulders have molecular weight values approximately twice that of the main peaks. In addition, the relative amounts of the high molecular weight impurities increase with increasing conversion. Although not quantified, it appears that PDMA synthesized using **1b**−**1d** contains approximately similar numbers of dead chains (see Figure 5). These side reactions can be avoided simply by limiting the conversion to less than 50% or by increasing the CTA/I ratio.

An interesting distinction of the DMA polymerization with **1a** is the significantly bimodal nature of the MWD as compared to CTAs **1b**−**1d**. For the polymerization with **1a**, it should also be noted that the two populations of chains appear to increase in molecular weight with conversion. This indicates both populations probably

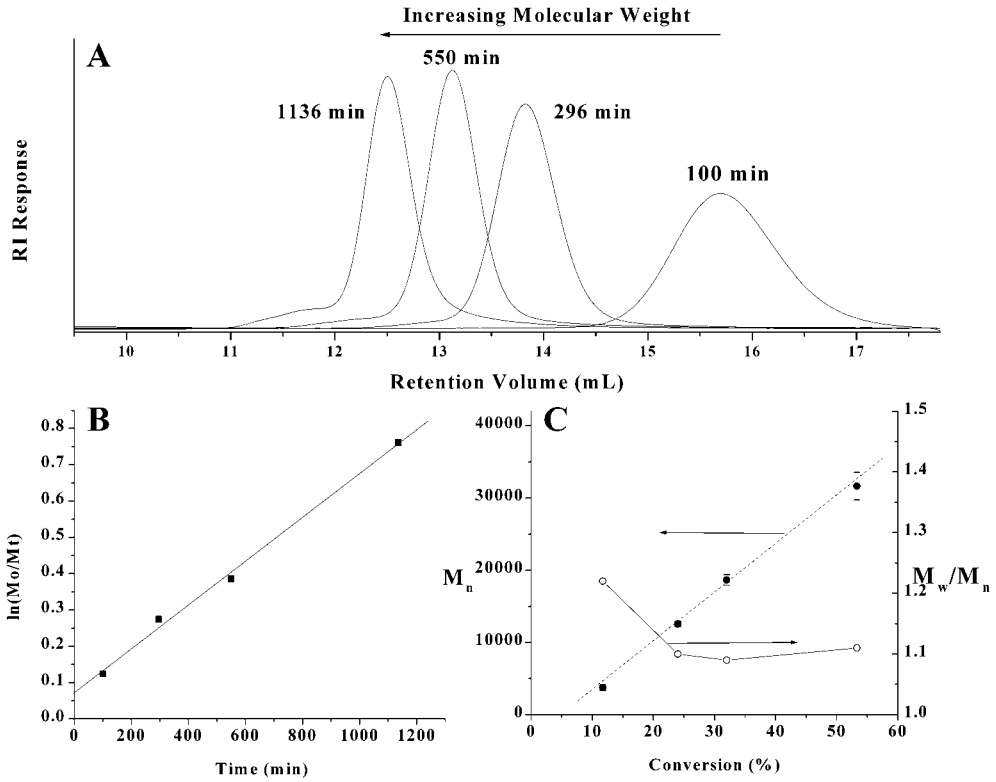

Figure 3. (A) SEC chromatograms for PDMA prepared with CTA **1c** (target MW = 40 000) in d_6-benzene at 60 °C using a CTA/I ratio of 5/1, [M] = 1.95 M, [CTA] = 4.27×10^{-3}, [I] = 8.46×10^{-4}. (B) Plot of $\ln(M_0/M_t)$ as a function of polymerization time. (C) Evolution of number-average molecular weight (●) and polydispersity (M_w/M_n) (○) with conversion.

Table 2. Data from the RAFT Polymerization of DMA with CTAs 1a−d (Target MW = 40 000) in d_6-Benzene (60 °C) Using a CTA/I Ratio of 5/1: [M] = 1.92 M, [CTA] = 4.81×10^{-3} M, [I] = 9.52×10^{-4} M

CTA	time (h)	% conv[a]	Mn_{Th}	Mn_{SEC}[b]	M_w/M_n
1a	14.5	80	32 000	50 700	1.22
1a	36.6	90	36 000	51 200	1.22
1a	66.5	97	38 800	53 200	1.24
1a	156.0	98	39 200	55 300	1.27
1a	181.5	98	39 200	59 700	1.23
1a	186.2	98	39 200	60 000	1.24
1b	8.1	59	23 600	35 800	1.12
1b	36.6	86	34 400	45 800	1.25
1b	66.5	95	38 000	54 600	1.24
1b	156.0	96	38 400	53 100	1.24
1b	181.5	96	38 400	53 400	1.25
1b	186.2	96	38 400	55 700	1.26
1c	19.0	78	31 200	35 200	1.14
1c	36.6	82	32 800	42 600	1.14
1c	66.5	93	37 200	48 500	1.19
1c	156.0	94	37 600	49 100	1.15
1c	181.5	95	38 000	50 000	1.18
1c	186.2	95	37 992	53 400	1.18
1d	10.9	67	26 800	39 400	1.15
1d	36.6	82	32 800	47 900	1.20
1d	66.5	96	38 400	49 600	1.24
1d	156.0	97	38 800	53 300	1.23
1d	181.5	98	39 200	53 350	1.24
1d	186.2	98	39 200	55 700	1.23

[a] As determined by ^{1}H NMR spectroscopy, recorded in d_6-benzene. [b] SEC in DMF at room temperature, at a flow rate of 0.5 mL/min, with x2 PL Mixed-D columns, PL UV-1200, Optilab RI, and DAWN EOS detectors.

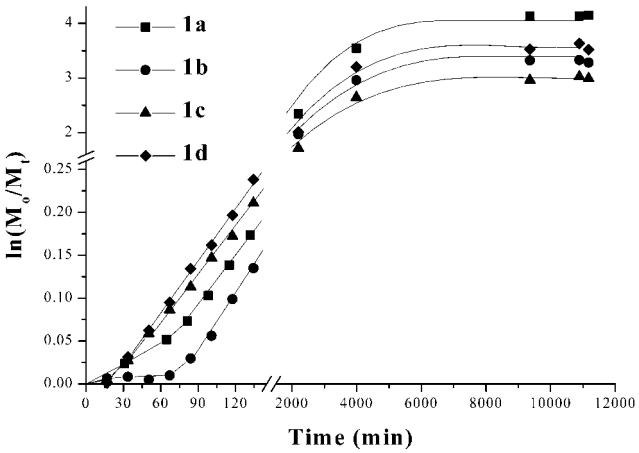

Figure 4. Plots of $\ln([M_0]/[M_t])$ vs t for DMA polymerizations in the NMR spectrometer in C_6D_6 (60 °C) using CTAs **1a**−**1d**.

contain active dithioester end groups. When comparing the relative amounts of each population at the various conversion values, it is evident that the lower molecular weight species is increasing faster than the higher molecular weight population. This may indicate the higher molecular weight population has fewer active end groups. One possible explanation for the significantly bimodal nature of PDMA synthesized using **1a** is that a number of chains are initiated early by primary AIBN-derived radicals. Assuming that the activation energy for fragmentation of the benzyl group and the PDMA polymer chain are similar, then statistically expulsion of either species should occur to roughly the same extent. However, whereas the PDMA macroradical can readily add to monomer, the benzyl group is a very poor initiating species, as discussed earlier, and is more likely to add to CTA. Eventually, however, the benzyl species will initiate polymerization, thus establishing the main RAFT equilibrium. However, there may already be a significant number of higher molecular weight AIBN-initiated PDMA chains by the time this equilibrium is established. This could, in principle, yield two distinct

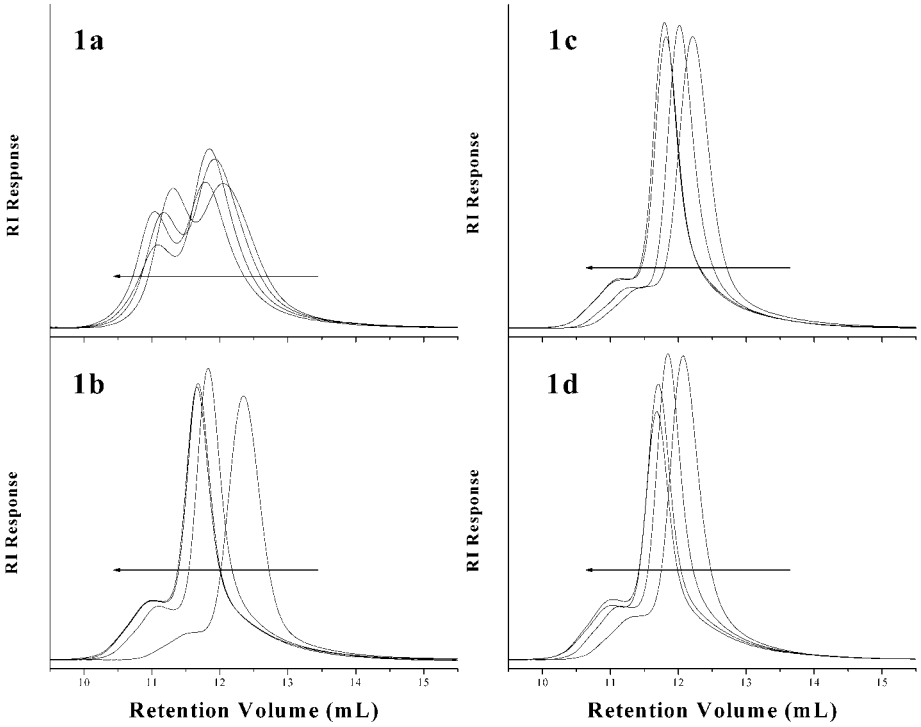

Figure 5. SEC traces for DMA polymerizations using CTA/I of 5/1 for CTAs **1a**−**1d** in C_6D_6 (60 °C) at extended polymerization times.

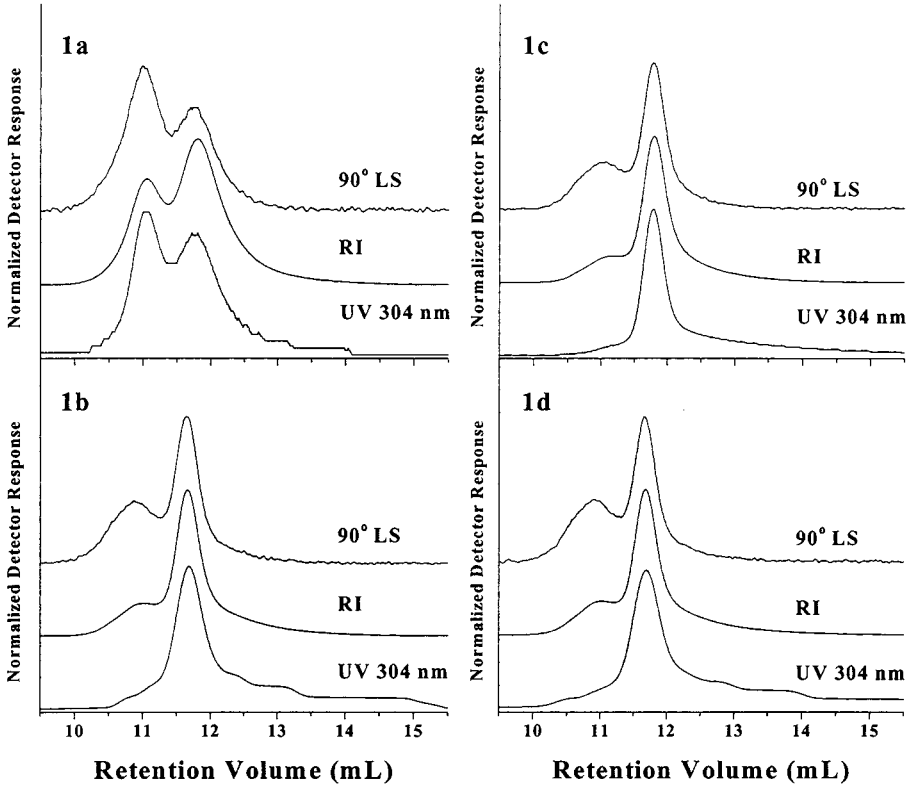

Figure 6. Comparison of light scattering (90°), RI, and UV detector responses of the SEC traces for PDMA using CTAs **1a**−**1d** (CTA/I = 5/1) in C_6D_6 (60 °C) after 181.5 h.

populations of "active" polymer chains—this will be discussed later in the paper.

In an attempt to further elucidate the nature of the higher molecular weight species observed in the SEC chromatograms at CTA/I ratios of 5/1, the online UV detector was utilized to monitor the presence (or absence) of dithioester species. Shown in Figure 6 are the RI, UV, and MALLS SEC chromatograms for PDMA synthesized using CTAs **1a**−**1d** (CTA/I ratio of 5/1) after 36.6 h. The presence of high molecular weight chains is clearly evident in the 90° MALLS detector response. The wavelength of the UV detector was tuned to 304

Table 3. Data from the RAFT Polymerization of DMA with CTAs 1a−d (Target MW = 40 000) in Benzene (60 °C) Using a CTA/I Ratio of 80/1: [M] = 1.94 M, [CTA] = 4.92 × 10^{-3} M, [I] = 6.28 × 10^{-5} M

CTA	CTA/I	time (h)	% conv[a]	Mn_{Th}	Mn_{SEC}[b]	M_w/M_n
1a	80	498	65	26 000	34 600	1.25
1b	80	498	56	22 400	33 000	1.11
1c	80	498	67	26 800	31 200	1.12
1d	80	498	55	22 000	35 600	1.22

[a] As determined by gravimetric analysis. [b] SEC in DMF at room temperature, at a flow rate of 0.5 mL/min, with x2 PL Mixed-D columns, PL UV-1200, Optilab RI, and DAWN EOS detectors.

nm, which corresponds to the λ_{max} of the π to π^* transition of the Ph−CS_2−Pn moiety. The absence of the high molecular weight shoulder (clearly observable in the RI and MALLS traces) in the UV trace is further evidence of bimolecular termination of polymer chains—these species will not contain dithioester end groups.

Despite the presence of the high molecular weight shoulders, the polydispersity indices are typically no greater than 1.25 (see Table 2), which indicates that all four CTAs meet at least one criterion for controlled polymerization. The lowest M_w/M_n values are observed for the more bulky CTAs **1b** and **1c**.

Influence of CTA/I Ratio. In an attempt to limit the number of dead polymer chains, the CTA/I ratio was increased from 5/1 to 80/1, while maintaining the targeted molecular weight of 40 000. The Mn_{SEC} and polydispersity indices for this series are given in Table 3. Examination of the data reveals that the polymerizations were significantly slower than those performed at a CTA/I ratio of 5/1. This is, of course, attributed to the increased probability of generated radicals to react with CTA or macro-CTA rather than monomer. As expected, the Mn_{Th} and Mn_{SEC} are in closer agreement than for the 5/1 ratios since the bimolecular termination events are less likely to occur. Likewise, the molecular weight distributions are significantly narrower.

The RI, UV, and MALLS SEC chromatograms for PDMA synthesized at the CTA/I ratio of 80/1 after a polymerization time of 498 h are shown in Figure 7. It is clearly obvious that increasing the CTA/I ratio (from 5/1 to 80/1) significantly improved the control over the respective polymerizations.

Although the observed molecular weight distribution for PDMA synthesized using **1a** is still bimodal, PDMAs synthesized using **1b**−**1d** are unimodal with little or no evidence of high molecular weight impurity. The best molecular weight control and narrowest molecular weight distribution were obtained using **1c**, with comparable results being obtained for **1b**. Given the low polydispersity (M_w/M_n = 1.12), coupled with the very small amount of high molecular weight impurity, PDMA synthesized using **1c** was subsequently employed as a "model" species for more involved chain-end analysis experiments using SEC.

The use of multiple detectors in SEC (RI, UV, and MALLS) facilitates the determination of the structure of each component in the molecular weight distribution. In particular, given the presence of UV-active chromophores (dithioester species), it is possible to monitor the chain-end structure across the entire molecular weight distribution.

To accurately determine the concentration of dithioester species across the molecular weight distribution, the extinction coefficient, ϵ, must be known. Using Beer's law, ϵ for the π−π^* transition of **1c** was determined in DMF using a UV spectrophotometer at 304 nm and was found to be 14 740 L/mol cm^{-1}. Using ϵ and the data from the UV chromatogram, it is possible to determine the concentration of the dithioester species (mol/L) at each volume slice. Similarly, using the refractive index increment (d*n*/d*c*) for PDMA and the RI chromatogram, the polymer concentration (g/L) can be determined. Dividing the polymer concentration by the dithioester concentration at each volume slice of the molecular weight distribution allows the UV molecular weight (MW_{uv}) to be determined. A comparison of MW_{uv} with the absolute molecular weight, as determined by the MALLS detector, provides a measure of the number of active chains, i.e., the number of PDMA chains containing dithioester end groups. The MW_{uv} of a PDMA homopolymer synthesized with **1c** (CTA/I = 80/1) was found to be 31 400 using the above method. This is in excellent agreement with the peak molecular weight of 31 700 as determined by MALLS. This close agreement thus confirms the presence of dithioester species on *all* polymer chains.

Thus, monitoring the UV profile across the molecular weight distribution provides an accurate way to follow changes in the dithioester end group distribution. In an ideal RAFT polymerization, the UV profile of the polymer chains should be the same throughout the molecular weight distribution since all chains should bear identical end groups. Using a similar procedure to the one described above, the UV SEC chromatogram of PDMA synthesized using **1a** was examined in an attempt to further understand the observed bimodality in the molecular weight distributions. For PDMA synthesized using **1a**, it was necessary to change the wavelength from 304 to 332 nm to avoid interfering absorbance of a shoulder for the phenyl chromophores.

Calculating the moles of polymer chains and the absorbance at each volume slice (using the RI/MALLS and UV detectors respectively), the absorptivity across the molecular weight distribution was determined using Beer's law. If *all* chains contain dithioester end groups, then the absorptivity should be constant across the entire molecular weight distribution. Figure 8b shows the change in absorptivity, at 332 nm, for PDMA synthesized using **1a**.

Even though the molecular weight distribution is bimodal, the absorptivity is fairly constant. This suggests that the high molecular weight species also contains dithioester end groups, and thus there exists two distinct populations of "active" chains. The higher molecular weight species does not appear to be due to products arising from bimolecular termination events. This is also supported in Figure 5, 1a (PDMA synthesized with **1a** at a CTA/I ratio of 5/1), where a clear increase in the molecular weight with time for both populations is observed, confirming both are active species. Given the poor initiating ability of the benzyl radical for DMA, the above analysis was repeated, but in this case at a wavelength of 276 nm—this allows us to monitor the benzyl initiating groups across the molecular weight distribution. At 276 nm, it was determined that both the phenyl group of the benzyl species and the dithioester contribute to the absorption profile. 276 nm was also chosen since the absorbance intensity at this wavelength is approximately equal to that observed purely for the dithioester end groups at 332 nm. Figure 8c shows the variation in absorptivity at 276 nm across the molecular weight distribution. It

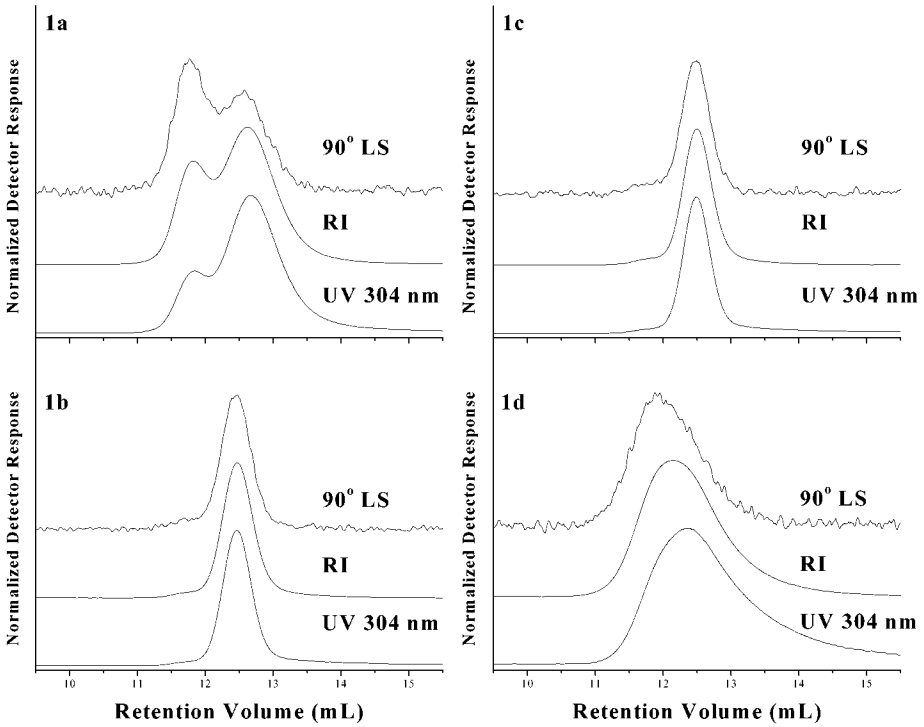

Figure 7. Comparison of light scattering (90°), RI, and UV detector responses of the SEC traces for PDMA using CTAs **1a**−**1d** (CTA/I = 80/1) in C_6H_6 (60 °C) after 498 h.

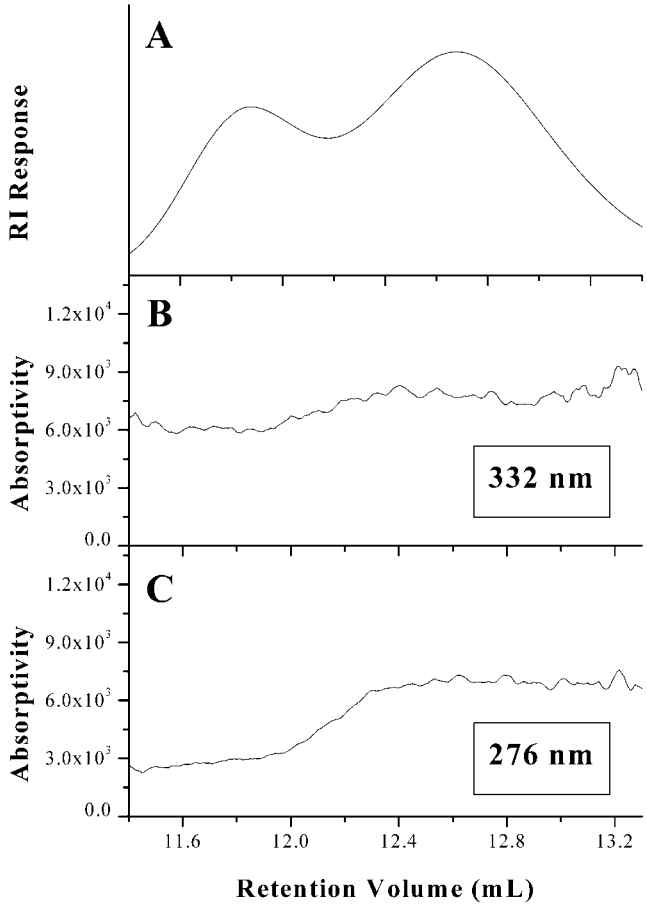

Figure 8. (A) SEC trace for PDMA using CTA **1a** (CTA/I = 80/1). (B) Plot of absorptivity at 332 nm vs retention volume. (C) Plot of absorptivity at 276 nm vs retention volume.

is clear that there is a significant decrease in the absorptivity for the higher molecular weight species. This is not due to a decrease in absorbance from the dithioester species since we have shown in Figure 8b that the absorptivity is fairly constant. Therefore, the decrease must be due to a lower contribution from the benzyl groups. This implies that the higher molecular weight chains were not all initiated by benzyl R groups. This supports our earlier hypothesis that some of the PDMA chains for **1a**-mediated polymerizations are initiated early on by AIBN-derived primary radicals and reach a significant molecular weight before completion of the RAFT preequilibrium.

Conclusions

Herein, we have reported the synthesis of two new RAFT CTAs, *N*,*N*-dimethyl-*s*-thiobenzoylthiopropionamide (**1c**) and *N*,*N*-dimethyl-*s*-thiobenzoylthioacetamide (**1d**), that were designed such that the R groups would be electronically and structurally similar to the propagating chain end of *N*,*N*-dimethylacrylamide (DMA) and were therefore expected to be highly efficient reinitiating species. Initial studies with **1c**, at a CTA/I ratio of 5/1, demonstrate the ability of this species to control the polymerization of DMA. Kinetic data indicates a first-order relationship for monomer conversion with time, while the molecular weight increases in a linear fashion with conversion. Also, polydispersity indices remain low throughout the course of the polymerization (M_w/M_n < 1.25).

A comparative study of the controlled polymerization of DMA using CTAs **1a**−**1d** indicates large differences in efficiency. At CTA/I ratios of 5/1, the kinetic data indicate rapid establishment of the main RAFT equilibrium for CTAs **1c** and **1d**, whereas significant retardation or inhibition is observed for **1a** and **1b**. These differences are rationalized in terms of the much poorer reinitiating abilities of the R fragments associated with **1a** and **1b**. Under these conditions all CTAs yield PDMA homopolymers containing high molecular weight impu-

rity. This impurity is attributed to products formed by the coupling of two PDMA macroradicals for CTAs **1b**−**1d** and also to the presence of two distinct "active" populations in the case of **1a**. However, the best control under these conditions is observed for **1c**.

We have subsequently demonstrated that the amount of high molecular weight impurity can be substantially reduced/eliminated simply by increasing the CTA/I ratio. Polymerizations conducted at a CTA/I ratio of 80/1 yield essentially unimodal molecular weight distributions for CTAs **1b** and **1c**, whereas **1a** yields PDMA with a bimodal distribution. The best molecular weight control and narrowest polydispersity are again observed for **1c** under these conditions.

The use of multiple detectors to analyze end groups (RI, UV, and MALLS) by size exclusion chromatography has allowed us to further elucidate the nature of the bimodality observed for the polymerizations conducted at 5/1 and the significantly bimodal nature of the **1a**-mediated polymerizations at both CTA/I ratios studied. We have demonstrated that the high molecular weight impurity, certainly for CTAs **1b**−**1d**, is due to bimolecular coupling reactions, as evidenced by the lack of any dithioester absorbance for this species. Although such reactions are of course also possible for **1a**-mediated polymerizations, end group analysis indicates that a significant proportion of the higher molecular weight species also contain dithioester end groups. This gives rise to two distinct active populations—also evidenced in SEC by the increase in molecular weight for both species with time.

Given the involved end group analysis in conjunction with the more conventional SEC analysis, we can therefore conclude that the novel acrylamido-based CTAs **1c** and **1d** are extremely effective in controlling the polymerization of DMA. This is due, we believe, to the structural and electronic similarity of the R groups to DMA, which results in highly efficient fragmentation/reinitiation and thus rapid establishment of the main RAFT equilibrium. The use of **1a** results in very poor overall control, whereas **1b** provides reasonable control but suffers form a large induction period, a result of its poor reinitiating ability.

Acknowledgment. We gratefully acknowledge the financial support for this research provided by Geltex Pharmaceuticals and the U.S. Department of Energy.

References and Notes

(1) (a) Le, T. P.; Moad, G.; Rizzardo, E.; Thang, S. H. PCT Int. Appl. WO 9801478 A1 980115. (b) Rizzardo, E.; Chiefari, J.; Mayadunne, R. T. A.; Moad, G.; Thang, S. H. *Controlled/Living Radical Polymerization, Progress in ATRP, NMP and RAFT*; Matyjaszewski, K., Ed.; ACS Symposium Series 768; American Chemical Society: Washington, DC, 2000; p 278.

(2) Chiefari, J.; Chong, Y. K.; Ercole, F.; Krstina, J.; Jeffery, J.; Le, T. P. T.; Mayadunne, R. T. A.; Meijs, G. F.; Moad, C. L.; Moad, G.; Rizzardo, E.; Thang, S. H. *Macromolecules* **1998**, *31*, 5559.

(3) Mayadunne, R. T. A.; Rizzardo, E.; Chiefari, J.; Krstina, J.; Moad, G.; Postma, A.; Thang, S. H. *Macromolecules* **2000**, *33*, 243.

(4) (a) Mayadunne, R. T. A.; Rizzardo, E.; Chiefari, J.; Chong, Y. K.; Moad, G.; Thang, S. H. *Macromolecules* **1999**, *32*, 6977. (b) Destarac, M.; Charmot, D.; Franck, X.; Zard, S. Z. *Macromol. Rapid Commun.* **2000**, *21*, 1035.

(5) (a) Taton, D.; Destarac, M.; Wilczewska, A.-Z. *Macromol. Rapid Commun.*, in press. (b) Francis, R.; Ajayaghosh, A. *Macromolecules* **2000**, *33*, 4699. (c) Ladavière, C.; Dörr, N.; Claverie, J. *Macromolecules* **2001**, *34*, 5370.

(6) Laus, M.; Papa, R.; Sparnacci, K.; Alberti, A.; Benaglia, M.; Macciantelli, D. *Macromolecules* **2001**, *34*, 7269.

(7) (a) Mitsukami, Y.; Donovan, M. S.; Lowe, A. B.; McCormick, C. L. *Macromolecules* **2001**, *34*, 2248. (b) Sumerlin, B. S.; Donovan, M. S.; Mitsukami, Y.; Lowe, A. B.; McCormick, C. L. *Macromolecules* **2001**, *34*, 6561.

(8) Bhandari, C. S.; Mahnot, U. S.; Sogani, N. C. *J. Prakt. Chem. (Leipzig)* **1971**, *313*, 849.

(9) (a) Goto, A.; Sato, K.; Tsujii, Y.; Fukuda, T.; Moad, G.; Rizzardo, Thang, S.; *Macromolecules* **2001**, *34*, 402. (b) Barner-Kowollik, C.; Quinn, J. F.; Morsley, D. R.; Davis, T. P. *J. Polym. Sci., Polym. Chem.* **2001**, *39*, 1353.

(10) Ganachaud, F.; Monteiro, M. J.; Gilbert, R. G.; Dourges, M.; Thang, S. H.; Rizzardo, E. *Macromolecules* **2000**, *33*, 6738.

(11) Barner-Kowollik, C.; Quinn, J. F.; Uyen Nguyen, T. L.; Heuts, J. P.; Davis, T. P. *Macromolecules* **2001**, *33*, 7849.

(12) Brandrup, J.; Immergut, E. H.; Grulke, E. A. *Polymer Handbook*, 4th ed.; John Wiley & Sons: New York, 1999.

(13) Moad, G.; Chiefari, J.; Chong, Y. K.; Krstina, J.; Mayadunne, R. T. A.; Postma, A.; Rizzardo, E.; Thang, S. H. *Polym. Int.* **2000**, *49*, 993.

MA0120714